


RESEARCH ARTICLE

Open Access



Structural determinants influencing halogen bonding: a case study on azinesulfonamide analogs of aripiprazole as 5-HT_{1A}, 5-HT₇, and D₂ receptor ligands

Krzysztof Marciniak^{1*} , Rafał Kurczab², Maria Książek³, Ewa Bębenek¹, Elwira Chrobak¹, Grzegorz Satała², Andrzej J. Bojarski², Joachim Kusz³ and Paweł Zajdel⁴

Abstract

A series of azinesulfonamide derivatives of long-chain arylpiperazines with variable-length alkylene spacers between sulfonamide and 4-arylpiperazine moiety is designed, synthesized, and biologically evaluated. In vitro methods are used to determine their affinity for serotonin 5-HT_{1A}, 5-HT₆, 5-HT₇, and dopamine D₂ receptors. X-ray analysis, two-dimensional NMR conformational studies, and docking into the 5-HT_{1A} and 5-HT₇ receptor models are then conducted to investigate the conformational preferences of selected serotonin receptor ligands in different environments. The bent conformation of tetramethylene derivatives is found in a solid state, in dimethyl sulfoxide, and as a global energy minimum during conformational analysis in a simulated water environment. Furthermore, ligand geometry in top-scored complexes is also bent, with one torsion angle in the spacer (τ_2) in synclinal conformation. Molecular docking studies indicate the role of halogen bonding in complexes of the most potent ligands and target receptors.

Keywords: Azinesulfonamides, Long-chain arylpiperazine, Aripiprazole, Crystal structure, Halogen bond

Introduction

Long-chain arylpiperazines (LCAPs) constitute one of the largest classes of serotonin (5-HT), and dopamine (D) receptor ligands, and exhibit diverse actions on the central nervous system (CNS) [1–4]. Among this vast group, we recently developed LCAP analogs of aripiprazole, with quinoline- or isoquinoline-sulfamoyl moieties, which displayed a 5-HT/D multi-receptor binding profile [5–8]. Structure–activity relationship studies have revealed that the observed receptor binding and functional profiles depend on the type of substituent in the arylpiperazine moiety, and the length and conformation of the aliphatic linker and the terminal fragment. Completing the characterization of this class of ligands, the selected compounds

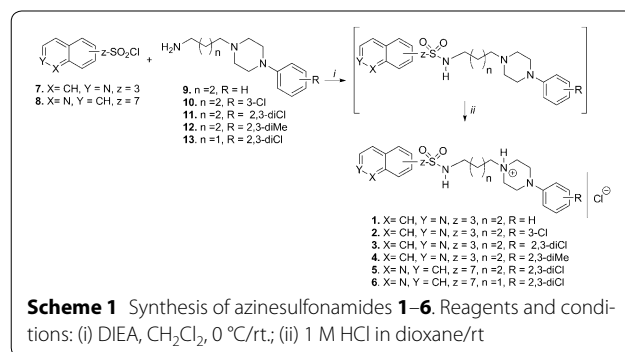
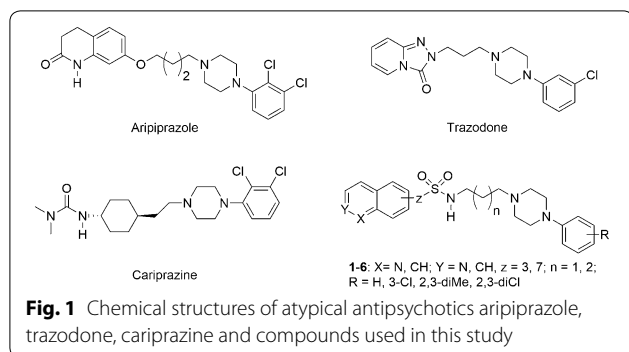
show potent antidepressant or antipsychotic activity with pro-cognitive properties [5–8].

In recent years, many research groups have explored monochloro- or dichloro-phenylpiperazine as a privileged structure for the optimization of CNS-active compounds providing with such psychotropic drugs as aripiprazole, trazodone, cariprazine [9–12] (Fig. 1). In the following years, the first reports were published on the engagement of halogen atoms in stabilization of the ligand–receptor complex within compounds targeting the central nervous system, especially 5-HT_{1A}, 5-HT₇, and D₂ receptors [13].

Some controversy has arisen concerning the role of the alkylene linker, usually composed of two to five carbon atoms as to whether it actively participates in binding or simply acts as a distance arm providing a chain [14]. Nevertheless, due to the highly flexible nature of a linker, various attempts have been made to determine the bioactive conformation of LCAPs.

*Correspondence: kmarciniec@sum.edu.pl

¹ Department of Organic Chemistry, Medical University of Silesia, 4 Jagiellońska Street, 41-200 Sosnowiec, Poland
Full list of author information is available at the end of the article



Assuming that active conformations of LCAPs are closely related to those in solution or in solid state, two-dimensional nuclear magnetic resonance (2D NMR) and crystallographic methods have often been applied to approximate the bioactive structure [15–20]. These 2D NMR studies indicate that compounds with an alkylene spacer can adopt extended, bent, or folded conformations [15–17]. In contrast, analysis of the Cambridge Structural Database (CSD) indicates that linear geometries are predominant (see Additional file 1: Table S1). Furthermore, molecular modeling simulations (conformational analysis and docking experiments) have provided equivocal results on the different bioactive conformations of LCAPs.

Extending studies on verification of the impact of halogen bond, alkylene linker length, and localization of the sulfonamide group in the azine moiety, a limited series of isoquinoline-sulfonamide derivatives of LCAP were designed (Fig. 1). Following our previous studies [5] suggesting the preferential position of the sulfonamide group in the β -position of the azinyl moiety, regardless of sulfonamide group localization in pyridine or benzene rings, the 3-isoquinolyl moiety was selected for the design of new aripiprazole analogs. Herein we report on the synthesis of selected azinesulfonamides and their X-ray structure analysis, followed by NMR experiments, and in silico molecular modeling. In doing so, we attempt to understand the conformational orientation of chemical sub-structures favorable for interaction with 5-HT_{1A} and 5-HT₇Rs.

Results and discussion

Source of compounds

Azinesulfonamide analogs of aripiprazole **1–6** were prepared according to previously reported procedures (Scheme 1) [5, 6].

The synthesis of compounds **1–6** was carried out by reaction of the primary amines (**9–13**) with 3-isoquinolinesulfonyl chloride (**7**) or 7-quinolinesulfonyl chloride (**8**) in the presence of Hunig's base. The azinesulfonyl chlorides **7** and **8** were prepared from

3-bromoisoquinoline or 7-chloroquinoline, respectively, according to the previously reported method [5]. For the pharmacological evaluation, free bases were converted into their water-soluble hydrochloride salts **1–6**. The spectroscopic data (NMR and MS) of compounds **3**, **5**, and **6** were identical to those previously reported [5].

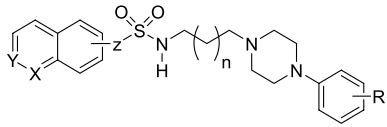
Structure–activity relationship studies

Following our previous studies [5], which suggest a preferential position of sulfonamide group in the β -position of the azinyl moiety (confirming the structural analogy for the dihydroquinolin-7-yl-2-one core in aripiprazole), 3-isoquinolyl moiety was selected to design the analogs of aripiprazole. In a series of new isoquinolinyl derivatives, we also focused our attention on the type of halogen substitution in a phenylpiperazine fragment to determine the role of the halogen bond in ligand complexes and target receptors.

The term “halogen bond” refers to the non-covalent interactions of halogen atoms X in one molecule with a negative site on another. X can be chlorine, bromine or iodine, but not fluorine. It is increasingly recognized that halogen bonding occurs in various biological systems and processes, and can be utilized effectively in drug design [21, 22]. Subsequently, regarding preliminary studies on the engagement of halogens in the interaction of LCAP derivatives with a partially rigidified alkylene spacer with serotonin receptors [8], our interest was focused on the impact of halogen in binding of compounds **2–6** with 5-HT_{1A} and 5-HT₇ receptors.

The unsubstituted analog **1** displayed low affinity for all tested receptors (Table 1). Introduction of chlorine in the 3-position increased receptors' affinity up to 3–12-fold (**1** vs **2**). These findings are in line with our previous study, and reveal that the presence of a chlorine atom in the 3-position stabilizes the ligand–receptor complex through the formation of a halogen bond with Thr5.39 residue of 5-HT_{1A} and 5-HT₇Rs [8]. Furthermore, introduction of a second chlorine atom in the 2-position of the phenylpiperazine yielded compound **3**. This modification

Table 1 Binding affinity of the investigated azinesulfonamides 1–6 for 5-HT_{1A}, 5-HT₆, 5-HT₇, and D₂ receptors

Compound				K _i (nM) ^a			
	Azinylyl	n	R	5-HT _{1A}	5-HT ₆	5-HT ₇	D ₂
1	3-isoquinolinylyl	2	H	304	1352	245	565
2	3-isoquinolinylyl	2	3-Cl	38	436	49	47
3^b	3-isoquinolinylyl	2	2,3-diCl	34	454	56	17
4	3-isoquinolinylyl	2	2,3-diMe	73	916	85	23
5^b	7-quinolinylyl	2	2,3-diCl	17	301	31	11
6^b	7-quinolinylyl	1	2,3-diCl	14	257	12	16
Aripiprazole	–	–	–	5.6	90	26	0.8

^a Mean K_i values (SEM ± 23%) based on three independent binding experiments

^b Data taken from Ref. [6]

did not substantially affect the receptor binding profile in comparison to its 3-chloro counterpart (**2** vs **3**), except for an increase in the affinity for D₂Rs. In contrast, replacement of chlorine atoms in the 2- and 3-positions with methyl groups (compound **4**) decreased the affinity for 5-HT_{1A}, and 5-HT₇Rs up to twofold (**3** vs **4**).

Subsequently, we compared the data obtained for 3-chloro- and 2,3-dimethyl derivatives (**2** and **4**, respectively) and unsubstituted phenylpiperazine analog **1** with those previously reported for their 2,3-dichloro analogs. A change of the 3-isoquinolinylyl fragment for 7-quinolinylyl yielded compound **5**, which displayed a two- to threefold higher affinity for 5-HT_{1A}, 5-HT₆, and 5-HT₇Rs, thus revealing the 7-quinolinylyl fragment as more favorable for interaction with 5-HT_{1A}Rs. Within the evaluated quinoline derivatives **5** and **6**, shortening of the butylene spacer to propylene one, had little influence on the receptor profile.

The binding data for D₂ receptors revealed that compound **1**, unsubstituted at the phenyl ring, displayed low affinity for D₂Rs with K_i equaling 565 nM (Table 1). Introduction of one chlorine atom in the 3-position increased affinity for D₂Rs 12-fold, and two chlorine atoms in the 2- and 3-positions increased affinity up to 33-fold. As found in our previous research [8], replacement of chlorine atoms with methyl substituents maintained affinity for D₂Rs at the same level. This could suggest a lower impact of halogen bonds, as they are less engaged in interaction with D₂Rs than in the case of 5-HT_{1A} and 5-HT₇Rs. Furthermore, it was found, that the 3-isoquinolinylyl fragment was less preferable than 7-quinolinylyl for interaction with D₂Rs (**4** vs **5**) and shortening of the alkylene linker (from 4 to 3 methylene units) maintained a high affinity for D₂Rs (**4** vs **6**).

Generally, the compounds selected for extended structural evaluation may be classified as multimodal serotonin and dopamine receptor ligands with high affinity for 5-HT_{1A}/5-HT₇ and D₂ receptors, and moderate to low affinity for 5-HT₆ receptors. Significantly, introduction of an azinesulfonamide group into the structure of LCAPs, decreased their affinity for D₂ receptors compared to aripiprazole [8].

Structural analysis

The Cambridge Structural Database (CSD version 5.39, November 2017 [23]) was used to search for compounds with the following queries: unsubstituted piperazine carbon atoms, no additional cyclic arrangements between aryl and piperazine moieties with ethylene, propylene, and butylene spacers. The search resulted in 36 hits (Additional file 1: Table S2). The piperazine ring in all structures deposited in the CSD adopts the chair conformation with substituents located equatorially. The mutual position of aryl and piperazine rings may be described simply by the torsional angle τ and/or dihedral angle ϕ between piperazine plain and the phenyl ring (Additional file 1: Figure S1). In the majority of *meta*- and *para*-substituted derivatives, the phenyl ring is more or less coplanar with piperazine (torsion angle values are grouped in the vicinity of 0° or 180°, while the dihedral angle is far from 90°). At the same time, all *ortho*-substituted compounds exhibit noncoplanar conformation. The spacers' conformations vary from fully extended to variously bent. Methylene chains predominantly adopt the extended form in the crystal. Meanwhile, in arylpiperazine salts piperazine nitrogen N1 is protonated and interacts with the respective anion through interionic hydrogen bonds. These interactions establish a salt bridge between the molecules, which plays a leading

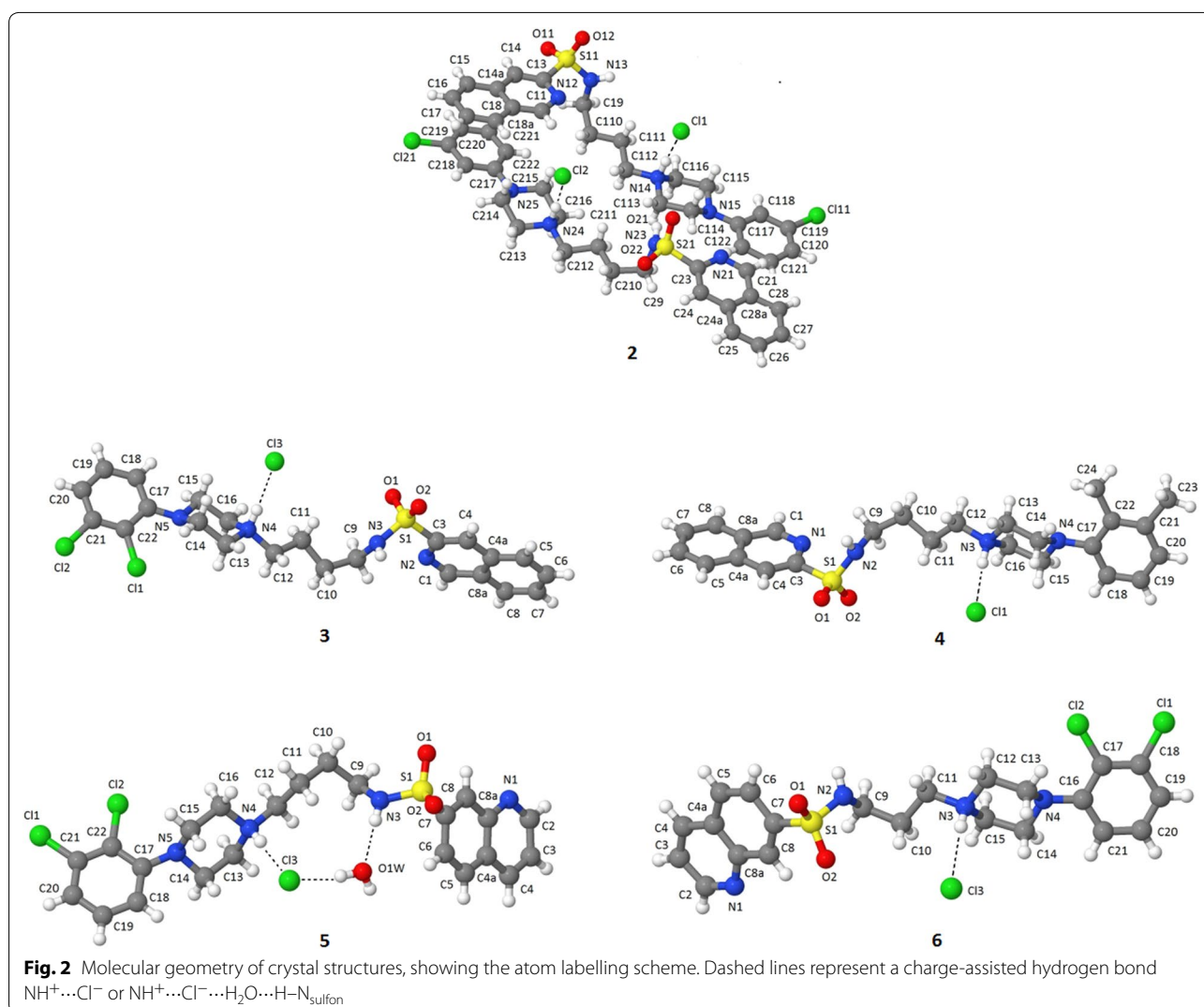
role in the discussed crystal architecture. In the case of solvent-free hydrochlorides, $\text{NH}^+\cdots\text{Cl}^-\cdots\text{H}-\text{C}_{\text{spacer}}$ interactions form a simple short bridge between more or less parallel molecules. Salt bridge elongation was observed in a number of structures containing water in the form of $\text{NH}^+\cdots\text{Cl}^-\cdots\text{H}_2\text{O}\cdots\text{H}-\text{C}_{\text{spacer}}$. Furthermore, these interactions caused important variation in the conformation of the alkylene spacer [20, 24].

Most of the above observations concerning the conformations of arylpiperazines collected in the CSD are self-evident for the five structures investigated in this paper. The main difference in the crystal structures of compounds 2–6 is the construction of salt bridges. Introduction of the $-\text{SO}_2-\text{NH}-$ sulfonamide fragment provides two strong proton acceptors and one strong proton donor which significantly change inter-ionic interaction in azinesulfonamides 2–6 compared to the crystal

structures deposited in the CSD. In the case of solvent-free hydrochlorides, the $\text{NH}^+\cdots\text{Cl}^-\cdots\text{H}-\text{N}_{\text{sulfon}}$ interactions form a simple short bridge. Salt bridge elongation, resulting from water participation, was observed in one structure in the form of $\text{NH}^+\cdots\text{Cl}^-\cdots\text{H}_2\text{O}\cdots\text{H}-\text{N}_{\text{sulfon}}$ in 5 (Fig. 2).

It should be mentioned that all derivatives 1–6 are highly resistant to crystallization and dissolve in most solvents; the glassy state is a dominant solid state for these derivatives. Therefore, we were fortunate to successfully obtain the monocrystals for five analogs of LCAPs. It should be pointed out that studying the structure nonsubstituted at phenyl ring analog 1 was also planned; however, owing to the crystal quality only a rough structure model was obtained.

In the structure of 2, two molecules were found in an independent unit, with the conformation of both



molecules being almost identical. Moreover, in the structure of hydrochloride **5**, besides the chlorine anion, a water molecule was also found. Significant geometrical parameters of the studied structures are summarized in Table 2.

In the crystal structures of compounds **2–6** the piperazine ring was in a common chair conformation (with the two N-substituents in equatorial positions) as indicated by deviations of nitrogen atoms in opposite directions from the plane defined by the ring carbons. The resulting distances were 0.63 and 0.64 Å for **2**, 0.73 and 0.64 Å for **3**, 0.73 and 0.64 Å for **4**, 0.72 and 0.62 Å for **5**, and 0.72 and 0.62 Å for **6**, respectively, with the second values referring to the protonated piperazine nitrogen, substituted equatorially by the alkylene linker. Accordingly, the inter-correlated position of piperazine and aromatic rings of the LCAPs may play a crucial role in ligand receptor recognition. The arylpiperazine moiety in the 2,3-disubstituted at phenyl ring azinesulfonamides **3–5** exhibits non-coplanar conformation with the main piperazine plane (formed by the atoms C13, C14, C15, and C16) and the phenyl inclined by $\phi = 47.1–62.8^\circ$. In the 3-substituted derivative **2**, the phenyl ring is more coplanar with the piperazine plane ($\phi = 20.6^\circ$) (Table 2). It is worth mentioning that in sulfonamides **5** and **6**, the most potent 5-HT_{1A} and 5-HT₇ receptor ligands, the angle between the piperazine plane and the phenyl ring reached its highest values (51.5° and 62.8° respectively). As a result, ability of the chlorine atom to stabilize the ligand–receptor (L–R) complex by the formation of stronger halogen bonds is increased compared with compounds **2** and **3**. Furthermore, the quinolinesulfonamide heterocyclic head and phenyl ring in compounds **5** and **6** were essentially planar, while in isoquinolinesulfonamides the phenyl and isoquinoline planes were almost perpendicular to each other in the crystals of **3** and **4** ($\phi = 81.6^\circ$ and 77.6° , respectively).

Special attention was placed upon the conformation of the alkylene spacer, due to its significant flexibility. Analysis of similar structures found in the CSD showed that an extended conformation of the spacer was favorable (see

Additional file 1: Table S1). The five new crystallographic structures obtained results that differed slightly from the protonated analogs of alkylarylpiperazines deposited in the CSD. In compound **6**, the *n*-propyl chain adopted a bent conformation gauche–trans–trans (for torsion angle see Table 2) and in the 2–5 conformation was not fully extended. The bending of the chain (gauche conformation) on the C9–C10 bond was essential for the obtained crystal structures (Fig. 3).

The supramolecular organization of the hydrochloride **2** was based mainly on different weak hydrogen bonds of the type C–H...Cl. Additionally one strong hydrogen bond between the nitrogen NH⁺ and Cl[−] anion was observed. The molecules were linked by weak hydrogen bonds between carbon atoms from the phenylpiperazine rings and oxygen atoms from the sulfonamide group. Additional file 1: Table S3 contains detailed characteristics of these interactions.

The solid-state conformations of azinesulfonamides **3** and **4** are stabilized by a system of intermolecular hydrogen bonds. The geometric parameters indicate that in the crystal structure of compounds **3** and **4**, molecules of the studied sulfonamides form chains, of the head-to-tail type stabilized by salt bridges of NH⁺...Cl[−]...H–N_{sulfon} (Additional file 1: Table S3).

Meanwhile, molecules of sulfonamide **5**, as well as sulfonamide **6**, were joined as a head-to-head type chain motif, with intermolecular distance equal to 6.91 Å. The

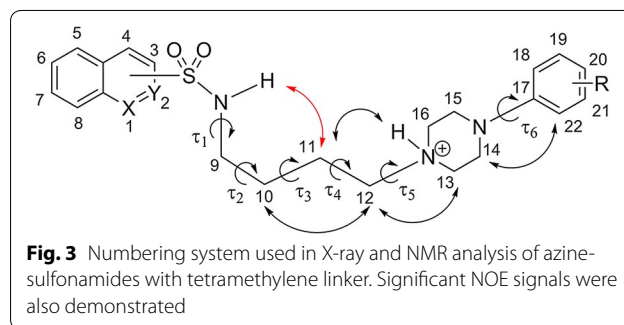


Table 2 Selected interatomic distances [Å] and dihedral angles [°]^a of the studied compounds

Compound	N ⁺ ...N _{sulfon}	τ ₁	τ ₂	τ ₃	τ ₄	τ ₅	τ ₆	Φ
2	5.47	−113.7	−69.0	179.4	−174.8	53.7	−147.5	20.6
3	5.48	−156.3	74.4	−170.5	−176.5	−49.5	159.2	47.1
4	5.48	−155.7	73.9	−171.4	−176.2	−50.5	158.8	48.0
5	5.00	−119.3	−65.1	−72.7	178.3	−53.7	−143.8	62.8
6	4.39	−102.7	−68.3	179.7	−55.1	−	154.6	51.5

^a For the definition of dihedral angles see Fig. 3

type of interaction that governs the crystal packing of the presented structure is strong hydrogen bonds, in which water molecules are involved. The observed hydrogen bond motives differ for sulfonamide **5** (Fig. 4), and the solvent molecule creates interesting patterns in the crystal lattice. Water molecules form the strong hydrogen bonds $\text{O}-\text{H}\cdots\text{Cl}^-\cdots\text{NH}^+$ and $\text{H}-\text{O}\cdots\text{H}-\text{N}_{\text{sulfon}}$. Moreover, in the crystal structure of **5**, water is a hydrogen bond donor with the quinolinesulfonamide oxygen atom acting as an acceptor (Additional file 1: Table S3).

The supramolecular organization of hydrochloride **6** is primarily governed by strong inter-ionic hydrogen bonds between the protonated arylpiperazine nitrogen, the chlorine anion located in the gap between extended

molecules and nitrogen of the sulfonamide group (Fig. 4). Thus, due to steric and geometrical complementarities, parallel molecules of **6** form chains of the head-to-head type, with an intermolecular distance equal to 6.82 Å. In this arrangement, molecules are joined by salt bridges of $\text{NH}^+\cdots\text{Cl}^-\cdots\text{H}-\text{N}_{\text{sulfon}}$ (graph set notation of $\text{C}_2^1(8)$) (Additional file 1: Table S3).

NMR studies

In the solid state, the compound exists in a bent conformation with the methylene bridging units in a synclinal–antiperiplanar–antiperiplanar–antiperiplanar arrangement for compounds **2–5**, and a synclinal–antiperiplanar–antiperiplanar arrangement for compound

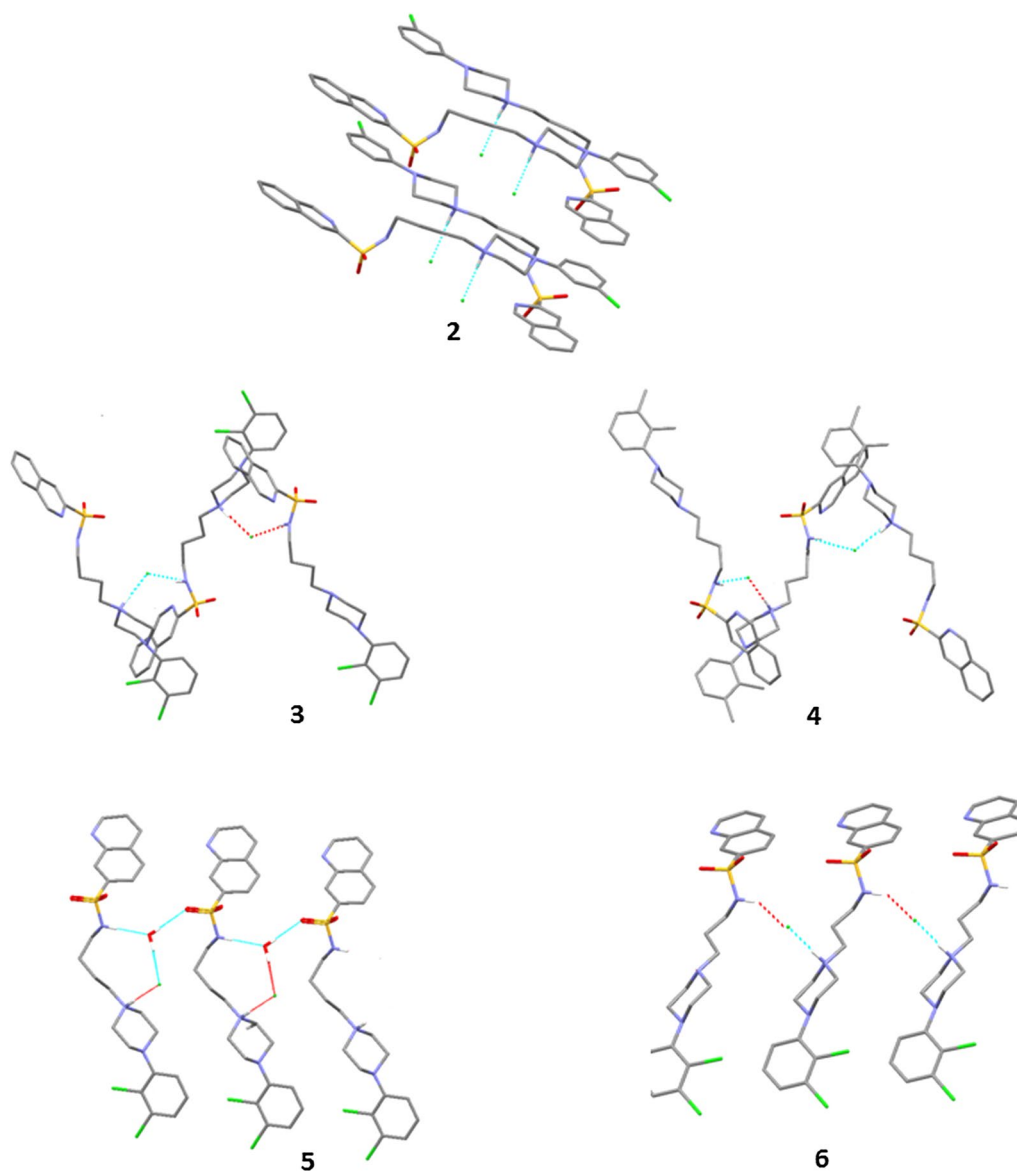


Fig. 4 Crystal packing of azinesulfonamides **2–6**. Hydrogen atoms not involved in the hydrogen bond patterns were removed for clarity

6. Since the chemical shift and multiplicity of two methylene groups (H-10 and H-11) in the tetramethylene bridging units can provide information about the conformational preferences of tested compounds, ^1H NMR studies for 2–5 were performed. In general, the ^1H NMR spectra of azinesulfonamides analyzed in DMSO solutions, were characterized by two multiplets separated by 0.25–0.27 ppm, assigned to the protons of two central methylene groups (H-10 and H-11) of the butyl chain. This might suggest the bent conformation, which is in agreement with previous observations [17, 25]. The above inferences were confirmed by the *nuclear Overhauser effect* (NOE). This experimental evidence for the conformations in solution of compounds 2–5 was provided by *rotating frame Overhauser effect spectroscopy* (ROESY) experiments conducted in DMSO; the significant NOE signals are indicated in Fig. 3. If the compounds were in their extended conformation, the interactions between the sulfonamide proton and H-11 would not be expected to exist. Alternatively, in a bent conformation the closer spatial arrangements of these protons could explain the observed NOE signals. In the obtained spectra, characteristic cross-peaks from the sulfonamide proton and methylene protons of the alkyl chain (H-11) were assigned the bent conformation. On the other hand, the appearance of weak interactions between H-9 and H-11 protons indicates the possibility of equilibrium between the bent and the extended conformation. However, the lack of interactions between the azine moiety and the phenyl protons (from arylpiperazine) definitely excludes the folded conformation of compounds and stacking interaction in solution.

Furthermore, 2D-NOE experiments confirmed the cross peaks for intramolecular interactions, are thus in agreement with bent conformations in solution. Molecular modeling studies of azinesulfonamides 2–6 were subsequently carried out with Gaussian 16 computer code. Conformational preferences were explored using the parameters for either the isolated “gas phase” or water continuum. Among the structures produced, the free energetically favored conformations indicated the methylene C9 and C10 bridging groups in a synclinal arrangement with aromatic portions far away from each other, consistent with NMR experimental data (Additional file 1: Table S4 and Figure S2). Higher energy extended structures were also generated, which were approximately 85 kJ/mol above the bent structures at most. This data constituted the basis for further molecular modeling and prediction of the ligands’ binding orientation to a receptor binding site.

Molecular modeling

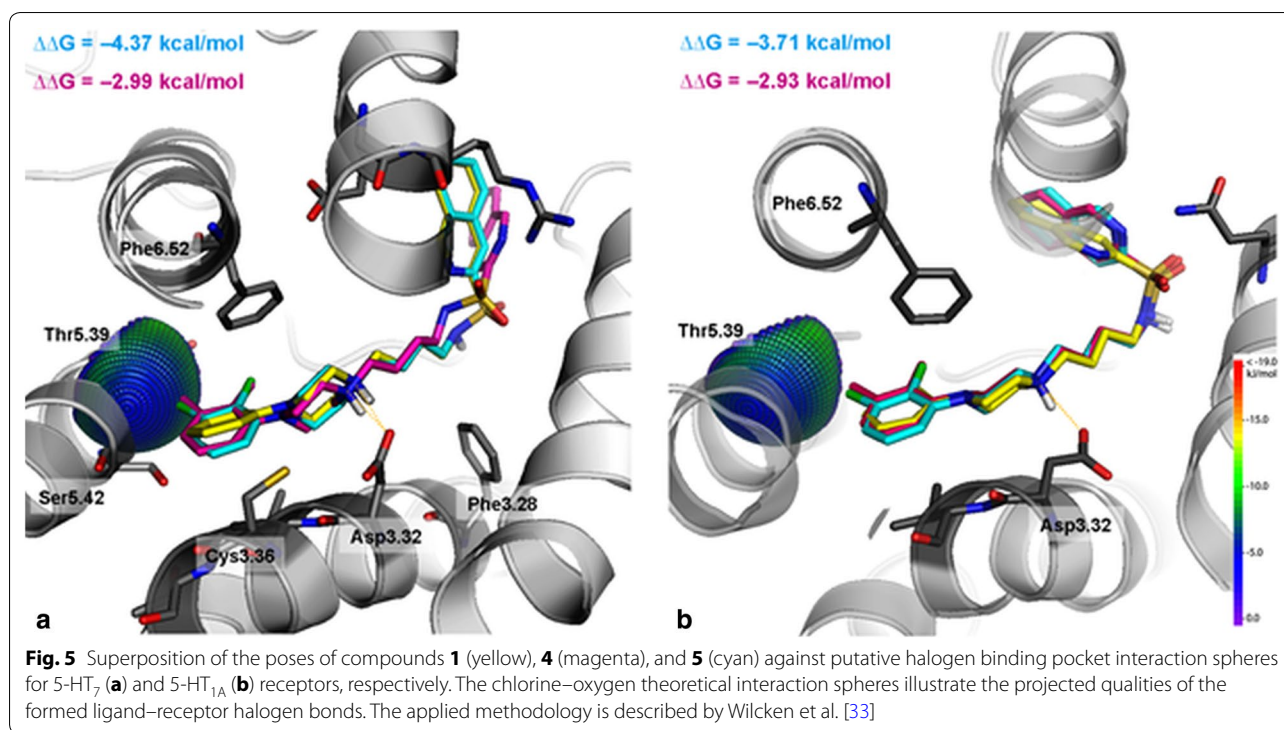
To complete the examination of the conformational preferences of the studied compounds, molecular docking of azinesulfonamides was performed with the use of recently developed 5-HT₇ and 5-HT_{1A} homology models, built on a dopaminergic D₃ receptor template (PDB ID: 3PBL) [13, 26–31]. Next, the combination of the QPLD with MM-generalized-born/surface area (MM/GBSA) calculations from the Schrödinger Suite was used to obtain ligand–receptor complexes, as this approach is suitable to describe the anisotropy of the electron density of halogen atoms, which is a key feature during halogen bond examination [32]. The obtained complexes (Fig. 5) exhibit highly consistent binding modes, involving a salt-bridge with Asp3.32 and interactions formed by the aromatic moiety of the arylpiperazine fragment (CH– π) with the side chain of Phe6.52. The higher affinity of 5 (with 2,3-dichloro substituent) for 5-HT₇ and 5-HT_{1A} than its unsubstituted analog 1 might be explained by the ability of chlorine to stabilize the ligand–receptor complex by the formation of a halogen bond (Cl...O distance = 3.38 Å, σ -hole angle = 177.6° for 5-HT₇R, and Cl...O distance = 3.62 Å, σ -hole angle = 167.9° for 5-HT_{1A}R, respectively) with the backbone carbonyl group of Thr5.39 (Fig. 5).

The change in binding affinities for compound 5 is probably related to the mutual orientation of the piperazine plane and the phenyl ring. In complexes of compound 5 with receptors, the angle between both rings maintains high values (57.4° for 5-HT_{1A} and 67.3° for 5-HT₇, respectively). Interestingly, in both receptors a higher increase in binding free energy ($\Delta\Delta G$) was noted for the dihalogenated (5) than dimethylated (4) analog of compound 1, indicating a significant role of halogen bonding in ligand–receptor interaction.

Among all of the docked poses, the bent conformations predominated and no extended arrangements were found (Additional file 1: Table S4). This is in general agreement with the parameters of related crystal structures as well as with NMR experimental data.

Conclusions

The present paper has reported the preparation and performance of biological and conformational studies for a small series of azinesulfonamide analogs of aripiprazole, with tri- and tetra-methylene spacers and phenylpiperazine substituted with chlorine and methyl groups. Among azine fragments, the 7-quinolinyl fragment was the most favorable for interaction with 5-HT_{1A}Rs. Moreover, the introduction of a chlorine atom or atoms into the phenyl ring significantly impacted the affinity for 5-HT_{1A} and 5-HT₇Rs. Furthermore, conformational studies (X-ray analysis and 2D NMR experiments) of the polymethylene



chain of LCAPs revealed that the bent conformation in a solid and in solutions is favorable. The above observations are compatible with the molecular modeling study performed for 2–6.

Docking analysis of the tested compounds suggest that all LCAPs were consequently docked in their bent conformations, with synclinal C9–C10 torsion, and that they bind to 5-HT_{1A} and 5-HT₇ receptors in a similar way. Our structural investigations organize knowledge about the conformational preferences of selected serotonin receptor ligands in different environments, and show that potentially bioactive conformations could be predicted by X-ray spectrometry and calculations using appropriate solvent simulated semi-empirical methods.

Experimental

Methods

Organic solvents (from Aldrich and Chempur) were of reagent grade and were used without purification.

Purity of the synthesized compounds was confirmed by TLC performed on Merck silica gel 60 F254 aluminium sheets (Merck, Darmstadt, Germany). Spots were detected by their absorption under UV light ($k = 254$ nm).

Analytical HPLC were run on a Waters Alliance HPLC instrument, equipped with a Chromolith SpeedROD column (4.6 × 50 mm). Standard conditions were eluent system A (water/0.1% TFA), system B (acetonitrile/0.1%

TFA). A flow rate of 5 mL/min and a gradient of (0–100) % B over 3 min were used. Detection was performed on a PDA detector. Retention times (tR) are given in minutes.

NMR Spectra were recorded on Bruker Ascend 600 spectrometer operating at 600.22 and 125.12 MHz for ¹H and ¹³C nuclei, respectively, in DMSO-*d*₆ solution. Two-dimensional ¹H–¹H (COSY and NOESY) and ¹H–¹³C (HSQC and HMBC) and NOE (ROESY) experiments were performed using standard Bruker software. J values are in hertz (Hz), and splitting patterns are designated as follows: s (singlet), brs (broad singlet) d (doublet), t (triplet), m (multiplet).

Mass spectrometry analyses—samples were prepared in acetonitrile/water (10/90 v/v) mixture. The LC/MS system consisted of a Waters Acquity UPLC, coupled to a Waters TQD mass spectrometer (electrospray ionization mode ESI-triple quadrupole (QQQ)). All other analyses were carried out using a Acquity UPLC BEH C18, 50 × 2.1 mm reversed-phase column. A flow rate of 0.3 mL/min and a gradient of (5–95) % B over 5 min was used. Eluent A: water/0.1% HCO₂H; eluent B: acetonitrile/0.1% HCO₂H. Nitrogen was used for both nebulizing and drying gas. LC/MS data were obtained by scanning the first quadrupole in 0.5 s in a mass range from 100 to 700 m/z; 10 scans were summed up to produce the final spectrum.

Elemental analyses were found within $\pm 0.4\%$ of the theoretical values. Melting points (mp) were determined with a Buchi apparatus and are uncorrected.

Column chromatography separations were carried out on column with Merck Kieselgel 60 or Aluminium oxide 90, neutral (70–230 mesh). Purification of compounds was performed on silica gel (irregular particles 40–63 μm , Merck Kieselgel 60).

General procedure for the preparation of compounds **1**, **2**, and **4**

The starting 1-(4-aminobutyl)-4-phenylpiperazine (**9**), 1-(4-aminobutyl)-4-(3-chlorophenyl)piperazine (**10**), 1-(4-aminobutyl)-4-(2,3-dichlorophenyl)piperazine (**11**), 1-(4-aminobutyl)-4-(2,3-dimethylphenyl)piperazine (**12**), and 1-(3-aminopropyl)-4-(2,3-dichlorophenyl)piperazine (**13**) were synthesized according to the Gabriel method. A mixture of the appropriate *N*-(ω -aminoalkyl)-phenylpiperazine (**9**–**13**) (1.0 mmol) in CH_2Cl_2 (7 mL) and DIEA (2.4 mmol) was cooled down (ice bath), and azinesulfonyl chloride **7** or **8** (1.2 mmol) was added at 0 °C in one portion. The reaction mixture was stirred for 6 h under cooling. Then, the solvent was evaporated and the sulfonamides were separated by column chromatography using SiO_2 and a mixture of $\text{CH}_2\text{Cl}_2/\text{MeOH} = 9/0.7$ or $9/0.5$, as an eluting system. Free bases were then converted into the hydrochloride salts by treatment of their solution in anhydrous ethanol with 1 M HCl in dioxane. The LC/MS of the identified compounds **1**–**6** exceeded purity of 98%.

N-(4-(4-phenyl)piperazin-1-yl)butyl)

isoquinoline-3-sulfonamide hydrochloride (**1**)

Yield 84%; m.p. 198–9 °C; ^1H NMR δ : 1.43–1.46 (m, 2H, H-10), 1.68–1.72 (m, 2H, H-11), 2.94 (td, 2H, $J = 6.6$ Hz, $J = 6.0$ Hz, H-9), 3.05–3.49 (m, 10H, H-12, H-13, H-14, H-15 and H-16), 7.07–7.18 (m, 5H, Ph), 7.88 (dd, 1H, $J = 8.4$ Hz, $J = 7.8$ Hz, H-6), 7.93–7.99 (m, 2H, H-7 and $-\text{SO}_2\text{NH}-$), 8.25–8.30 (m, 2H, H-5 and H-8), 8.52 (s, 1H, H-4), 9.49 (s, 1H, H-1), 10.95 (brs, 1H, $-\text{CH}_2\text{NH}^+(\text{CH}_2\text{CH}_2)_2\text{N}-$); ^{13}C NMR δ : 20.8 (C-11), 27.1 (C-10), 42.7 (C-9), 48.3 (C-14 and C-15), 51.8 (C-13 and C-16), 55.3 (C-12), 120.3 (C-4), 125.5 (Ph), 128.3 (Ph), 128.4 (C-5), 128.5 (C-3), 128.6 (Ph), 129.4 (C-8), 130.5 (C-6), 132.6 (C-7), 135.4 (C-4a), 139.3 (Ph), 151.5 (C-8a), 153.9 (C-1).

N-(4-(4-(3-chlorophenyl)piperazin-1-yl)butyl)

isoquinoline-3-sulfonamide hydrochloride (**2**)

Yield 89%; m.p. 246–7 °C; ^1H NMR δ : 1.43–1.45 (m, 2H, H-10), 1.67–1.71 (m, 2H, H-11), 2.94 (td, 2H, $J = 6.6$ Hz, $J = 6.0$ Hz, H-9), 3.05–3.49 (m, 10H, H-12, H-13, H-14, H-15 and H-16), 6.87 (d, 1H, $J = 7.2$ Hz, Ph), 6.95 (d, 1H,

$J = 7.8$ Hz, Ph), 7.07 (s, 1H, Ph), 7.25 (dd, 1H, $J = 7.8$ Hz, $J = 7.2$ Hz, Ph), 7.90 (dd, 1H, $J = 8.4$ Hz, $J = 7.8$ Hz, H-6), 7.93–7.98 (m, 2H, H-7 and $-\text{SO}_2\text{NH}-$), 8.26–8.33 (m, 2H, H-5 and H-8), 8.53 (s, 1H, H-4), 9.48 (s, 1H, H-1), 10.06 (brs, 1H, $-\text{CH}_2\text{NH}^+(\text{CH}_2\text{CH}_2)_2\text{N}-$); ^{13}C NMR δ : 22.6 (C-11), 27.1 (C-10), 42.7 (C-9), 45.4 (C-14 and C-15), 50.9 (C-13 and C-16), 55.4 (C-12), 114.7 (Ph), 115.8 (Ph), 120.3 (C-4 and Ph), 128.4 (C-5), 128.5 (C-8), 129.4 (C-3), 130.5 (Ph), 131.1 (C-6), 132.6 (C-7), 134.4 (Ph), 135.4 (C-4a), 147.9 (Ph), 151.5 (C-8a), 154.0 (C-1).

N-(4-(4-(2,3-dimethylphenyl)piperazin-1-yl)butyl) isoquinoline-3-sulfonamide hydrochloride (**4**)

Yield 86%; m.p. 215–6 °C; ^1H NMR δ : 1.44–1.48 (m, 2H, H-10), 1.71–1.75 (m, 2H, $J = 6.6$ Hz, H-11), 2.15 (s, 3H, $-\text{CH}_3$), 2.21 (s, 3H, $-\text{CH}_3$), 2.93 (td, 2H, $J = 6.6$ Hz, $J = 6.0$ Hz, H-9), 3.08–3.46 (m, 10H, H-12, H-13, H-14, H-15 and H-16), 6.87–6.91 (m, 2H, Ph), 7.04–7.09 (m, 1H, Ph), 7.86–7.99 (m, 3H, H-6, H-7 and $-\text{SO}_2\text{NH}-$), 8.25–8.31 (m, 2H, H-5 and H-8), 8.53 (s, 1H, H-4), 9.49 (s, 1H, H-1), 10.93 (brs, 1H, $-\text{CH}_2\text{NH}^+(\text{CH}_2\text{CH}_2)_2\text{N}-$); ^{13}C NMR δ : 14.1 ($-\text{CH}_3$), 20.7 ($-\text{CH}_3$), 20.8 (C-11), 27.1 (C-10), 42.7 (C-9), 48.9 (C-14 and C-15), 51.7 (C-13 and C-16), 55.4 (C-12), 116.9 (Ph), 120.3 (C-4), 125.9 (Ph), 126.3 (Ph), 128.4 (C-5), 128.5 (C-3), 129.4 (C-8), 130.5 (C-6), 131.0 (Ph), 132.6 (C-7), 135.4 (C-4a), 138.1 (Ph), 150.3 (Ph), 151.5 (C-8a), 153.9 (C-1).

X-ray crystal structures determination

Crystals of **2**–**6** were obtained by slow evaporation of the solvent under ambient conditions from ethanol: water mixture in ratio of 5:1.

X-ray diffraction data were collected using SuperNova diffractometer with Cu $K\alpha$ radiation ($\lambda = 1.54184$ Å) for crystal **2** and with Mo $K\alpha$ radiation ($\lambda = 0.71073$ Å) for crystals **3**–**6**, with the CrysAlisPro software [34]. Data were processed with the same program. Experiments were performed at 100 K excepting crystal of **4**, which was measured at room temperature. The phase problem was solved by direct methods with SHELXS-97 [35]. The model parameters were refined by full-matrix least-squares on F^2 using SHELXL-2014/7 [35]. All non-hydrogen atoms were refined anisotropically. Hydrogen atoms were introduced to all structures by appropriate rigid body constraints (AFIX 23, AFIX 43 or AFIX 137) with temperature factors $U_{\text{iso}}(\text{H})$ equal to 1.2Ueq(C) for aromatic and methylene hydrogen atoms or 1.5Ueq(C) for methyl hydrogen atoms. Hydrogen atoms which take part in the hydrogen bonds were located in the calculated positions and then freely refined. Due to severely disordered solvent in crystal of **2**, the SQUEEZE program was used [36]. All crystallographic data for presented structures are shown in Additional file 1: Table S5. The figures

showing asymmetric units were made with Jmol [37]. The figure presenting structural motives were made with Mercury [38].

In vitro evaluation

Cell culture and preparation of cell membranes for radioligand binding assays

HEK293 cells with stable expression of human 5-HT_{1A}, 5-HT₆, 5-HT_{7b} and D_{2L} receptors (prepared with the use of Lipofectamine 2000) were maintained at 37 °C in a humidified atmosphere with 5% CO₂ and grown in Dulbecco's Modified Eagle Medium containing 10% dialyzed fetal bovine serum and 500 µg/ml G418 sulfate. For membrane preparation, cells were subcultured in 150 cm² flasks, grown to 90% confluence, washed twice with prewarmed to 37 °C phosphate buffered saline (PBS) and pelleted by centrifugation (200g) in PBS containing 0.1 mM EDTA and 1 mM dithiothreitol. Prior to membrane preparation, pellets were stored at – 80 °C.

Radioligand binding assays

Cell pellets were thawed and homogenized in 10 volumes of assay buffer using an Ultra Turrax tissue homogenizer and centrifuged twice at 35,000g for 15 min at 4 °C, with incubation for 15 min at 37 °C in between. The composition of the assay buffers was as follows: for 5-HT_{1A}R: 50 mM Tris HCl, 0.1 mM EDTA, 4 mM MgCl₂, 10 µM pargyline and 0.1% ascorbate; for 5-HT₆R: 50 mM Tris HCl, 0.5 mM EDTA and 4 mM MgCl₂, for 5-HT_{7b}R: 50 mM Tris HCl, 4 mM MgCl₂, 10 µM pargyline and 0.1% ascorbate; for dopamine D_{2L}R: 50 mM Tris HCl, 1 mM EDTA, 4 mM MgCl₂, 120 mM NaCl, 5 mM KCl, 1.5 mM CaCl₂ and 0.1% ascorbate. All assays were incubated in a total volume of 200 µl in 96-well microtitre plates for 1 h at 37 °C, except 5-HT_{1A}R which were incubated at room temperature. The process of equilibration was terminated by rapid filtration through Unifilter plates with a FilterMate Unifilter 96-Harvester (PerkinElmer). The radioactivity bound to the filters was quantified on a Microbeta TopCount instrument (PerkinElmer, USA). For competitive inhibition studies the assay samples contained as radioligands (PerkinElmer, USA): 2.5 nM [³H]-8-OH-DPAT (135.2 Ci/mmol) for 5-HT_{1A}R; 2 nM [³H]-LSD (83.6 Ci/mmol) for 5-HT₆R; 0.8 nM [³H]-5-CT (39.2 Ci/mmol) for 5-HT₇R or 2.5 nM [³H]-raclopride (76.0 Ci/mmol) for D_{2L}R. Non-specific binding was defined with 10 µM of 5-HT in 5-HT_{1A}R and 5-HT₇R binding experiments, whereas 10 µM of methiothepine or 10 µM of haloperidol were used in 5-HT₆R and D_{2L} assays, respectively. Each compound was tested in triplicate at 7 concentrations (10⁻¹⁰–10⁻⁴ M). The inhibition

constants (*K_i*) were calculated from the Cheng–Prusoff equation [39]. Results were expressed as means of at least two separate experiments.

Computational details

Geometry optimization

Ab initio calculations of the studied azinesulfonamides, using crystallographic data as starting point, were carried out with the Gaussian 16 (revision A.03) computer code [40] at the density functional theory (DFT, Becke3LYP [41]) level of theory using the 6–311+G(d,p) basis sets. The conformational behavior of these systems in water was examined using the CPCM solvation method [42, 43].

Molecular docking

3-Dimensional structures of the ligands were prepared using LigPrep v3.6 [44], and the appropriate ionization states at pH 7.4 ± 1.0 were assigned using Epik v3.4 [45]. The Protein Preparation Wizard was used to assign the bond orders, appropriate amino acid ionization states and to check for steric clashes. The receptor grid was generated (OPLS3 force field [46]) by centering the grid box with a size of 12 Å on Asp3.32 residue. Docking was performed by quantum-polarized ligand docking (QPLD) procedure [47] involves the QM-derived ligand atomic charges in the protein environment at the B3PW91/cc-pVTZ level. Only ten best poses per ligand returned by the procedure were considered.

Binding free energy calculations

MM/GBSA (Generalized-Born/Surface Area) was used to calculate the binding free energy based on the ligand–receptor complexes generated by the QPLD procedure. The ligand poses were minimized using the local optimization feature in Prime, the flexible residue distance was set to 4.0 Å from a ligand pose, and the ligand charges obtained in the QPLD stage were used. The energies of complexes were calculated with the OPLS3 force field and Generalized-Born/Surface Area continuum solvent model. To assess the influence of a given substituent on the binding, the ΔΔG was calculated as a difference between binding free energy (ΔG) of unsubstituted at phenyl ring sulfonamide 1 and investigated analogs 3, 4, and 5.

Plotting interaction spheres for halogen bonding

To visualize (plotting interaction spheres) the possible contribution of halogen bonding to ligand–receptor complexes, the halogen bonding web server was used (access Oct 01, 2017, <http://www.halogenbonding.com/>).

Additional file

Additional file 1: Figure S1. Histograms of population of different arylpiperazine salts conformations. **Figure S2.** Low-energy conformation of the studied compounds in aqueous medium. **Table S1.** Conformation of arylpiperazine derivatives with polymethylene spacer (H-N+(CH₂)_n-N) in the crystal state (n=3 and 4). **Table S2.** Conformation of phenyl ring and piperazine moiety in arylpiperazine derivatives with polymethylene spacer [H-N+(CH₂)_n-X] in the crystal state (n=2-4). **Table S3.** Strong and weak hydrogen bonds geometry for structures 2-6 [Å and °]. **Table S4.** Optimized dihedral angles [°] of the studied compounds. **Table S5.** Crystal data and structure refinement.

Authors' contributions

KM synthesized the title compounds and was responsible for each stage of the preparation of this manuscript, including carrying out the literature study, designing synthetic schemes and figures, preparing the crystals of tested compounds, and performing NMR experiments as well as geometry optimization. RK was responsible for the docking study and contributed to writing this manuscript. JK collected the X-ray data. The crystal structures were solved and refined by MK. GS carried out radioligand binding assays under the direct supervision of JB. EB, EC and PZ contributed to writing this paper. All authors read and approved the final manuscript.

Author details

¹ Department of Organic Chemistry, Medical University of Silesia, 4 Jagiellońska Street, 41-200 Sosnowiec, Poland. ² Department of Medicinal Chemistry, Institute of Pharmacology, Polish Academy of Sciences, 12 Smętna Street, 31-343 Krakow, Poland. ³ Institute of Physics, University of Silesia, 4 Uniwersytecka Street, 40-007 Katowice, Poland. ⁴ Department of Medicinal Chemistry, Jagiellonian University Medical College, 9 Medyczna Street, 30-688 Krakow, Poland.

Acknowledgements

This work was supported by Grant KNW-1-015/K/7/O from Medical University of Silesia, Katowice, Poland. Calculations have been carried out using resources provided by Wrocław Centre for Networking and Supercomputing (<http://wcss.pl>), Grant No. 382.

Competing interests

The authors declare that they have no competing interests.

Availability of data and materials

All data are fully available without restriction.

Consent for publication

The authors declare that the copyright belongs to the journal.

Ethics approval and consent to participate

Not applicable.

Publisher's Note

Springer Nature remains neutral with regard to jurisdictional claims in published maps and institutional affiliations.

Received: 29 March 2018 Accepted: 28 April 2018

Published online: 11 May 2018

References

- Volk B, Gacsalyi I, Pallagi K, Poszawacz L, Gyonos I, Szabo E, Bako T, Spedding M, Simig G, Szenasi G (2011) Optimization of (aryl)piperazinylbutyl oxindoles exhibiting selective 5-HT₇ receptor antagonist activity. *J Med Chem* 54:6657–6669
- Butini S, Gemma S, Campiani G, Franceschini S, Trotta F, Borriello M, Ceres N, Ros S, Sanna Coccone S, Bernetti M, De Angelis M, Brindisi M, Nacci V, Fiorini I, Novellino E, Cagnotto A, Mennini T, Sandager-Nielsen K, Andreasen JT, Scheel-Kruger J, Mikkelsen JD, Fattorusso C (2009) Discovery of a new class of potential multifunctional atypical antipsychotic agents targeting dopamine D₃ and serotonin 5-HT_{1A} and 5-HT_{2A} receptors: design, synthesis, and effects on behavior. *J Med Chem* 52:151–169
- Leopoldo M, Berardi F, Colabufo NA, De Giorgio P, Lacivita E, Perrone R, Tortorella V (2002) Structure–affinity relationship study on *N*-[4-(4-aryl)piperazin-1-yl]butyl]arylcarboxamides as potent and selective dopamine D₃ receptor ligands. *J Med Chem* 45:5727–5735
- Zajdel P, Partyka A, Marciniec K, Bojarski AJ, Pawłowski M, Wesolowska A (2014) Quinoline- and isoquinoline-sulfonamide analogs of aripiprazole: novel antipsychotic agents? *Future Med Chem* 6:1–19
- Zajdel P, Marciniec K, Maślankiewicz A, Grychowska K, Satała G, Duszyńska B, Lenda T, Siwek A, Nowak G, Partyka A, Wróbel D, Jastrzębska-Więsek M, Bojarski AJ, Wesolowska A, Pawłowski M (2013) Antidepressant and antipsychotic activity of new quinoline- and isoquinoline-sulfonamide analogs of aripiprazole targeting serotonin 5-HT_{1A}/5-HT_{2A}/5-HT₇ and dopamine D₂/D₃ receptors. *Eur J Med Chem* 60:42–50
- Zajdel P, Marciniec K, Maślankiewicz A, Satała G, Duszyńska B, Bojarski AJ, Partyka A, Jastrzębska-Więsek M, Wróbel D, Wesolowska A, Pawłowski M (2012) Quinoline- and isoquinoline-sulfonamide derivatives of LCAP as potent CNS multi-receptor-5-HT_{1A}/5-HT_{2A}/5-HT₇ and D₂/D₃/D₄-agents: the synthesis and pharmacological evaluation. *Bioorg Med Chem* 20:1545–1556
- Zajdel P, Kos T, Marciniec K, Satała G, Canale V, Kamiński K, Hołuj M, Lenda T, Koralewski R, Bednarski M, Nowiński L, Wójcikowski J, Daniel WA, Nikiforuk A, Nalepa I, Chmielarz P, Kuśmierczyk J, Bojarski AJ, Popik P (2018) Novel multi-target azinesulfonamides of cyclic amine derivatives as potential antipsychotics with pro-social and pro-cognitive effects. *Eur J Med Chem* 60:42–50
- Partyka A, Kurczab R, Canale V, Satała G, Marciniec K, Pasierb A, Jastrzębska-Więsek M, Pawłowski M, Wesolowska A, Bojarski AJ, Zajdel P (2017) The impact of the halogen bonding on D₂ and 5-HT_{1A}/5-HT₇ receptor activity of azinesulfonamides of 4-[(2-ethyl)piperidinyl-1-yl]phenylpiperazines with antipsychotic and antidepressant properties. *Bioorg Med Chem* 25:3638–3648
- Banala AK, Levy BA, Khatri SS, Furman CA, Roof RA, Mishra Y, Griffin SA, Sibley DR, Luedtke RR, Newman AH (2011) *N*-(3-fluoro-4-(4-(2-methoxy or 2,3-dichlorophenyl)piperazine-1-yl)butyl)arylcarboxamides as selective dopamine D₃ receptor ligands: critical role of the carboxamide linker for D₃ receptor selectivity. *J Med Chem* 54:3581–3594
- Shapiro DA, Renock S, Arrington E, Chiodo LA, Liu LX, Sibley DR, Roth BL, Mailman R (2003) Aripiprazole, a novel atypical antipsychotic drug with a unique and robust pharmacology. *Neuropsychopharmacology* 28:1400–1411
- Khouzam HR (2017) A review of trazodone use in psychiatric and medical conditions. *J Postgrad Med* 129:140–148
- Veselinović T, Paulzen M, Gründer G (2013) Cariprazine, a new, orally active dopamine D_{2/3} receptor partial agonist for the treatment of schizophrenia, bipolar mania and depression. *Expert Rev Neurother* 13:1141–1159
- Canale V, Guzik P, Kurczab R, Verdier P, Satała G, Kubica B, Pawłowski M, Martinez J, Subra G, Bojarski AJ, Zajdel P (2014) Solid-supported synthesis, molecular modeling, and biological activity of long-chain arylpiperazine derivatives with cyclic amino acid amide fragments as 5-HT₇ and 5-HT_{1A} receptor ligands. *Eur J Med Chem* 78:10–22
- Caliendo G, Santagada V, Perissutti E, Fiorino F (2005) Derivatives as 5HT_{1A} receptor ligands—past and present. *Curr Med Chem* 12:1721–1753
- Nishimura T, Igarashi J, Sunagawa M (2001) Conformational analysis of tandospirone in aqueous solution: lead evolution of potent dopamine D₄ receptor ligands. *Bioorg Med Chem Lett* 11:1141–1144
- Siracusa MA, Salerno L, Modica MN, Pittalà V, Romeo G, Amato ME, Nowak M, Bojarski AJ, Mereghetti I, Cagnotto A, Mennini T (2008) Synthesis of new arylpiperazinylalkylthiobenzimidazole, benzothiazole, or benzoxazole derivatives as potent and selective 5-HT_{1A} serotonin receptor ligands. *J Chem Med* 51:4529–4538
- Lewgond W, Bojarski AJ, Szczesio M, Olczak A, Glowka ML, Mordalski S, Stanczak A (2011) Synthesis and structural investigation of some pyrimido[5,4-*c*]quinolin-4(3*H*)-one derivatives with a long-chain arylpiperazine moiety as potent 5-HT_{1A/2A} and 5-HT₇ receptor ligands. *Eur J Med Chem* 46:3348–3361

18. Nanubolu JB, Sridhar B, Ravikumar K, Cherukuvada S (2013) Adaptability of aripiprazole towards forming isostructural hydrogen bonding networks in multi-component salts: a rare case of strong O—H...O ↔ weak C—H...O mimicry. *CrystEngComm* 15:4321–4334
19. Karolak-Wojciechowska J, Fruzinski A, Kowalska T, Kowalski P (2003) Crystal structure of 4-(3-chlorophenyl)-1-[4-(4-oxoquinazolin-3(4*H*)-yl)-butyl]piperazin-1-ium chloride trihydrate, (C₂₂H₂₆ClN₄O)Cl 3H₂O. *Z Kristallogr New Cryst Struct* 218:191–193
20. Karolak-Wojciechowska J, Fruzinski A, Mokrosz MJ (2001) Structure and conformational analysis of new arylpiperazines containing *n*-butyl chain. *J Mol Struct THEOCHEM* 542:47–56
21. Clark T, Hennemann M, Murray JS, Politzer P (2001) Halogen bonding: the sigma-hole. In: Proceedings of "Modeling interactions in biomolecules II", Prague, September 5th–9th, 2005. *J Mol Model*. 13:291–296
22. Wilcken R, Zimmermann MO, Lange A, Zahn S, Boeckler FM (2012) Using halogen bonds to address the protein backbone: a systematic evaluation. *J Comput Aided Mol Des* 26:935–945
23. Groom CR, Bruno IJ, Lightfoot MP, Ward SC (2016) The Cambridge structural database. *Acta Cryst B* 72:171–179
24. Karolak-Wojciechowska J, Mrozek A, Fruzinski A, Szczesio M, Kowalski P, Kowalska T (2010) H-bond pattern in arylpiperazine structures. Structures of *cis* and *trans* 2-[4-[4-(2-methoxyphenyl)piperazin-1-yl]but-2-enyl]isoindoline-1,3-diones and their hydrochloride salts. *J Mol Struct* 979:144–151
25. Norman MH, Minick JD, Rigdon GC (1996) Effect of linking bridge modifications on the antipsychotic profile of some phthalimide and isoindolinone derivatives. *J Med Chem* 39:149–157
26. Canale V, Partyka A, Kurczab R, Krawczyk M, Kos T, Satała G, Kubica B, Jastrzębska-Więsek M, Wesolowska A, Bojarski AJ, Popik P, Zajdel P (2017) Novel 5-HT₇R antagonists, arylsulfonamide derivatives of (aryloxy)propyl piperidines: add-on effect to the antidepressant activity of SSRI and DRI, and pro-cognitive profile. *Bioorg Med Chem* 25:2789–2799
27. Intagliata S, Modica MN, Pittalà V, Salerno L, Siracusa MA, Cagnotto A, Salmona M, Kurczab R, Romeo E (2017) New *N*- and *O*-arylpiperazinylalkyl pyrimidines and 2-methylquinazolines derivatives as 5-HT₇ and 5-HT_{1A} receptor ligands: synthesis, structure-activity relationships, and molecular modeling studies. *Bioorg Med Chem* 25:1250–1259
28. Kurczab R, Canale V, Zajdel P, Bojarski AJ (2016) An algorithm to identify target-selective ligands—a case study of 5-HT_{7/5}-HT_{1A} receptor selectivity. *PLoS ONE* 11:e0156986
29. Canale V, Kurczab R, Partyka A, Satała G, Słoczyńska K, Kos T, Jastrzębska-Więsek M, Siwek A, Pękala E, Bojarski AJ, Wesolowska A, Popik P, Zajdel P (2016) *N*-Alkylated arylsulfonamides of (aryloxy)ethyl piperidines: 5-HT₇ receptor selectivity versus multireceptor profile. *Bioorg Med Chem* 24:130–139
30. Canale V, Kurczab R, Partyka A, Satała G, Lenda T, Jastrzębska-Więsek M, Wesolowska A, Bojarski AJ, Zajdel P (2016) Towards new 5-HT₇ antagonists among arylsulfonamide derivatives of (aryloxy)ethyl-alkyl amines: multiobjective based design, synthesis, and antidepressant and anxiolytic properties. *Eur J Med Chem* 108:334–336
31. Canale V, Kurczab R, Partyka A, Satała G, Witek J, Jastrzębska-Więsek M, Pawłowski M, Bojarski AJ, Wesolowska A, Zajdel P (2015) Towards novel 5-HT₇ versus 5-HT_{1A} receptor ligands among LCAPs with cyclic amino acid amide fragments: design, synthesis, and antidepressant properties. Part II. *Eur J Med Chem* 92:202–211
32. Kurczab R (2017) The evaluation of QM/MM-driven molecular docking combined with MM/GBSA calculations as a halogen-bond scoring strategy. *Acta Crystallogr Sect B Struct Sci Cryst Eng Mater* 73:188–194
33. Wilcken R, Zimmermann MO, Lange A, Joerger AC, Boeckler FM (2013) Principles and applications of halogen bonding in medicinal chemistry and chemical biology. *J Med Chem* 56:1363–1388
34. CrysAlisPro Software System (2015) Version 1.171.38.41. Rigaku oxford diffraction. <http://www.rigaku.com>
35. Sheldrick GM (2015) Crystal structure refinement with *SHELXL*. *Acta Crystallogr Sect C Struct Chem* C71:3–8
36. Spek A (2015) PLATON SQUEEZE: a tool for the calculation of the disordered solvent contribution to the calculated structure factors. *Acta Crystallogr Sect C Struct Chem* C71:9–18
37. Willighagen E, Howard M (2007) Fast and scriptable molecular graphics in web browsers without Java3D. *Nat Preced*. <https://doi.org/10.1038/npre.2007.50.1>
38. Macrae CF, Edgington PR, McCabe P, Pidcock E, Shields GP, Taylor R, Towler M, van de Streek J (2006) Visualization and analysis of crystal structures. *J Appl Crystallogr* 39:453–457
39. Cheng Y, Prusoff W (1973) Relationship between the inhibition constant (K_i) and the concentration of inhibitor which causes 50 per cent inhibition (I₅₀) of an enzymatic reaction. *Biochem Pharmacol* 22:3099–3108
40. Frisch MJ, Trucks GW, Schlegel HB, Scuseria GE, Robb MA, Cheeseman JR, Scalmani G, Barone V, Petersson GA, Nakatsuji H, Li X, Caricato M, Marenich AV, Bloino J, Janesko BG, Gomperts R, Mennucci B, Hratchian HP, Ortiz JV, Izmaylov AF, Sonnenberg JL, Williams-Young D, Ding F, Lipparini F, Egidi F, Goings J, Peng B, Petrone A, Henderson T, Ranasinghe D, Zakrzewski VG, Gao J, Rega N, Zheng G, Liang W, Hada M, Ehara M, Toyota K, Fukuda R, Hasegawa J, Ishida M, Nakajima T, Honda Y, Kitao O, Nakai H, Vreven T, Throssell K, Montgomery JA, Peralta JE, Ogliaro F, Bearpark MJ, Heyd JJ, Brothers EN, Kudin KN, Staroverov VN, Keith TA, Kobayashi R, Normand J, Raghavachari K, Rendell AP, Burant JC, Iyengar SS, Tomasi J, Cossi M, Millam JM, Klene M, Adamo C, Cammi R, Ochterski JW, Martin RL, Morokuma K, Farkas O, Foresman JB, Fox DJ (2016) Gaussian 16, Revision A. 03. 2016. Gaussian Inc., Wallingford CT
41. Stephens PJ, Devlin FJ, Chablowski CF, Frisch M (1994) Ab initio calculation of vibrational absorption and circular dichroism spectra using density functional force fields. *J Phys Chem* 98:11623–11627
42. Klamt A, Schuurman G (1993) COSMO: a new approach to dielectric screening in solvents with explicit expressions for the screening energy and its gradient. *J Chem Soc Perkin Trans* 2:799–805
43. Cossi M, Rega N, Scalmani G, Barone V (2003) Energies, structures, and electronic properties of molecules in solution with the C-PCM solvation model. *J Comput Chem* 24:669–681
44. Schrödinger Release 2018-1, LigPrep, Schrödinger, LLC, New York. 2018
45. Schrödinger Release 2018-1, Epik, Schrödinger, LLC, New York. 2018
46. Harder E, Damm E, Maple J, Wu C, Reiboul M, Xiang JY, Wang L, Lupyan D, Dahlgren MK, Knight JL, Kaus JW, Cerutti DS, Krilov G, Jorgensen WL, Abel R, Friesner RA (2016) OPLS3: a force field providing broad coverage of drug-like small molecules and proteins. *J Chem Theor Comput* 12:281–296
47. Schrödinger Release 2018-1: Schrödinger Suite 2018-1 QM-Polarized Ligand Docking protocol; Glide, Schrödinger, LLC, New York, 2016; Jaguar, Schrödinger, LLC, New York, 2016; QSite, Schrödinger, LLC, New York, 2018

Submit your manuscript to a SpringerOpen® journal and benefit from:

- Convenient online submission
- Rigorous peer review
- Open access: articles freely available online
- High visibility within the field
- Retaining the copyright to your article

Submit your next manuscript at ► springeropen.com